Article

Steric and Electronic Properties of N-Heterocyclic Carbenes (NHC): A Detailed Study on Their Interaction with Ni(CO)

Reto Dorta, Edwin D. Stevens, Natalie M. Scott, Chiara Costabile, Luigi Cavallo, Carl D. Hoff, and Steven P. Nolan

J. Am. Chem. Soc., **2005**, 127 (8), 2485-2495• DOI: 10.1021/ja0438821 • Publication Date (Web): 02 February 2005

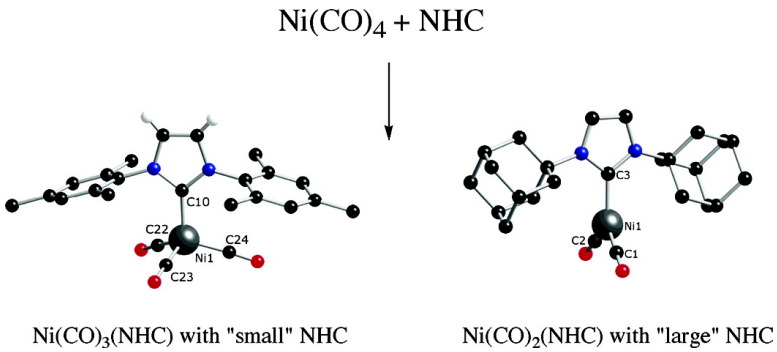

More About This Article

Additional resources and features associated with this article are available within the HTML version:

- Supporting Information
- Links to the 61 articles that cite this article, as of the time of this article download
- Access to high resolution figures
- Links to articles and content related to this article
- Copyright permission to reproduce figures and/or text from this article

View the Full Text HTML

J|A|C|S
ARTICLES
Published on Web 02/02/2005

Steric and Electronic Properties of N-Heterocyclic Carbenes (NHC): A Detailed Study on Their Interaction with $Ni(CO)_4$

Reto Dorta,[†] Edwin D. Stevens,[†] Natalie M. Scott,[†] Chiara Costabile,[‡] Luigi Cavallo,[‡] Carl D. Hoff,[§] and Steven P. Nolan*,[†]

Contribution from the Department of Chemistry, University of New Orleans, New Orleans, Louisiana 70148, Dipartimento di Chimica, Università di Salerno, Baronissi, SA 84081, Italy, and Department of Chemistry, University of Miami, Coral Gables, Florida 33124

Received October 7, 2004; E-mail: snolan@uno.edu

Abstract: N-heterocyclic carbene ligands IMes (**1**), SIMes (**2**), IPr (**3**), SIPr (**4**), and ICy (**5**) react with $Ni(CO)_4$ to give the saturated tricarbonyl complexes $Ni(CO)_3$(IMes) (**8**), $Ni(CO)_3$(SIMes) (**9**), $Ni(CO)_3$(IPr) (**10**), $Ni(CO)_3$(SIPr) (**11**), and $Ni(CO)_3$(ICy) (**12**), respectively. The electronic properties of these complexes have been compared to their phosphine analogues of general formula $Ni(CO)_3(PR_3)$ by recording their ν_{CO} stretching frequencies. While all of these NHCs are better donors than tertiary phosphines, the differences in donor properties between ligands **1**−**5** are surprisingly small. Novel, unsaturated $Ni(CO)_2$(IAd) (**13**) and $Ni(CO)_2$(I^{t}Bu) (**14**) compounds are obtained from the reaction of $Ni(CO)_4$ with IAd (**6**) and I^{t}Bu (**7**). Complexes **13** and **14** are highly active toward substitution of the NHC as well as the carbonyl ligands. This has allowed the determination of Ni−C(NHC) bond dissociation energies and the synthesis of various unsaturated Ni(0) and Ni(II) complexes. Computational studies on compounds **8**−**14** are in line with the experimental findings and show that IAd (**6**) and I^{t}Bu (**7**) are more bulky than IMes (**1**), SIMes (**2**), IPr (**3**), SIPr (**4**), and ICy (**5**). Furthermore, a method based on $\%V_{bur}$ values has been developed for the direct comparison of steric requirements of NHCs and tertiary phosphines. Complexes **8**−**14**, as well as $NiCl(C_3H_5)$(I^{t}Bu) (**16**) and $NiBr(C_3H_5)$(I^{t}Bu) (**17**), have been characterized by X-ray crystallography.

Introduction

Since the isolation and crystallographic characterization of stable N-heterocyclic carbenes (NHCs) by Arduengo et al.,[1] increasing attention has been focused on using these compounds as ancillary ligands for transition-metal complexes. Recent developments in homogeneous catalysis have shown that NHCs are attractive alternatives to the ubiquitous tertiary phosphine ligands.[2] Several beneficial uses of NHC-modified organometallic systems in ruthenium-mediated olefin metathesis,[3] iridium-catalyzed hydrogenation and hydrogen transfer,[4] platinum-catalyzed hydrosilylation,[5] or C−C coupling reactions using carbene complexes of palladium[6] are now well recognized. In all of these catalytic processes, monocarbene ligands have emerged as the most promising systems. The most widely used NHCs of this class are represented in Figure 1.

Although some spectroscopic studies have revealed the close relationship of NHCs with phosphine ligands,[7] detailed electronic and steric investigations on this ligand class have not been reported and remain largely unquantified. The importance of quantifying steric and electronic effects of ligands has been recognized in pioneering studies by Tolman on phosphines and has had a major impact on the development of new and improved phosphine ligands for catalysis.[8] In the case of the NHC ligands shown in Figure 1, surprising differences in catalytic activities of the corresponding metal catalysts have already been observed, but could not be rationalized or explained

[†] University of New Orleans.
[‡] Università di Salerno.
[§] University of Miami.

(1) Arduengo, A. J., III; Harlow, R. L.; Kline, M. *J. Am. Chem. Soc.* **1991**, *113*, 361−363.
(2) (a) Bourissou, D.; Guerret, O.; Gabbai, F. P.; Bertrand, G. *Chem. Rev.* **2000**, *100*, 39−91. (b) Herrmann, W. A. *Angew. Chem., Int. Ed.* **2002**, *41*, 1290−1309. (c) Yong, B. S.; Nolan, S. P. *Chemtracts: Org. Chem.* **2003**, *16*, 205−227.
(3) (a) Weskamp, T.; Schattenmann, W. C.; Spiegler, M.; Herrmann, W. A. *Angew. Chem., Int. Ed.* **1998**, *37*, 2490−2493. (b) Huang, J.; Stevens, E. D.; Nolan, S. P.; Petersen, J. L. *J. Am. Chem. Soc.* **1999**, *121*, 2674−2678. (c) Scholl, M.; Ding, S.; Lee, C. W.; Grubbs, R. H. *Org. Lett.* **1999**, *1*, 953−956. For reviews, see: (d) Jafarpour, L.; Nolan, S. P. *Adv. Organomet. Chem.* **2001**, *46*, 181−222. (e) Jafarpour, L.; Nolan, S. P. *J. Organomet. Chem.* **2001**, *617*, 17−27. (f) Trnka, T. M.; Grubbs, R. H. *Acc. Chem. Res.* **2001**, *34*, 18−29. (g) Fürstner, A. *Angew. Chem., Int. Ed.* **2000**, *39*, 3013−3043.
(4) (a) Lee, H. M.; Jiang, T.; Stevens, E. D.; Nolan, S. P. *Organometallics* **2001**, *20*, 1255−1258. (b) Hillier, A. C.; Lee, H. M.; Stevens, E. D.; Nolan, S. P. *Organometallics* **2001**, *20*, 4246−4252. (c) Vasquez-Serrano, L. D.; Owens, B. T.; Buriak, J. M. *Chem. Commun.* **2002**, 2518−2519.
(5) Markò, I. E.; Stérin, S.; Buisine, O.; Mignani, G.; Branlard, P.; Tinant, B.; Declerq, J.-P. *Science* **2002**, *298*, 204−208.
(6) (a) Grasa, G. A.; Viciu, M. S.; Huang, J.; Nolan, S. P. *J. Org. Chem.* **2001**, *66*, 7729−7737. (b) Grasa, G. A.; Viciu, M. S.; Huang, J.; Zhang, C.; Trudell, M. L.; Nolan, S. P. *Organometallics* **2002**, *21*, 2866−2873. (c) Viciu, M. S.; Germaneau, R. F.; Nolan, S. P. *Org. Lett.* **2002**, *4*, 4053−4056. (d) Navarro, O.; Kelly, R. A., III; Nolan, S. P. *J. Am. Chem. Soc.* **2003**, *125*, 16194−16195.
(7) (a) Öfele, K.; Herrmann, W. A.; Mihalios, D.; Elison, M.; Herdtweck, E.; Scherer, W.; Mink, J. *J. Organomet. Chem.* **1993**, *459*, 177−184. (b) Denk, K.; Sirsch, P.; Herrmann, W. A. *J. Organomet. Chem.* **2002**, *649*, 219−224. (c) Chianese, A. R.; Li, X.; Janzen, M. C.; Faller, J. W.; Crabree, R. H. *Organometallics* **2003**, *22*, 1663−1667.
(8) Tolman, C. A. *Chem. Rev.* **1977**, *77*, 313−348.

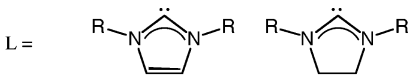

R	L	L
2,4,6-trimethylphenyl	IMes (**1**)	SIMes (**2**)
2,6-diisopropylphenyl	IPr (**3**)	SIPr (**4**)
cyclohexyl	ICy (**5**)	
adamantyl	IAd (**6**)	
tert-butyl	I^{t}Bu (**7**)	

Figure 1. Common unsaturated and saturated NHCs.

experimentally. Furthermore, although NHC ligands are believed to strongly bind to late-transition metals, extensive experimental determination of metal−NHC bonding energies has not been carried out so far.

To achieve a deeper understanding of the fundamental steric and electronic factors characterizing the NHC ligand class and to afford a direct comparison with the large array of data available for tertiary phosphine ligands, we report here our studies on the substitution reaction involving $Ni(CO)_4$ and NHC ligands **1**−**7**. Most of these ligands give rise to the expected, saturated complexes of general composition $Ni(CO)_3(NHC)$. The electronic properties of these NHCs are compared to those of tertiary phosphine ligands. The most bulky NHC ligands lead to the isolation of novel, three-coordinate nickel carbonyl systems. These unsaturated complexes have allowed, for the first time, the experimental determination of bond dissociation energies for this ligand class. All new Ni(0)−NHC complexes were characterized by X-ray crystallography. In combination with computational studies, this has enabled the establishment of a method for the direct comparison of steric requirements of the NHC and phosphine ligand classes. Furthermore, reactivity studies showed that while the saturated complexes are essentially inert toward displacement of the NHC and the carbonyl ligands, the unsaturated analogues are highly reactive toward ligand substitution and oxidative addition of substrates. Some of the results herein have been previously published in a communication.[9]

Results and Discussion

Synthesis and Structure of Saturated $Ni(CO)_3(NHC)$. Reaction of a hexane or THF solution containing IMes (**1**), SIMes (**2**), IPr (**3**), SIPr (**4**), or ICy (**5**) with a slight excess of $Ni(CO)_4$ led to immediate evolution of CO. Subsequent workup gave the saturated complexes $Ni(CO)_3$(IMes) (**8**), $Ni(CO)_3$(SIMes) (**9**), $Ni(CO)_3$(IPr) (**10**), $Ni(CO)_3$(SIPr) (**11**), and $Ni(CO)_3$(ICy) (**12**) as off-white or beige solids in high yield (eq 1).

$$Ni(CO)_4 + NHC \rightarrow Ni(CO)_3(NHC) + CO \qquad (1)$$

NHC = IMes for **8**, SIMes for **9**, IPr for **10**, SIPr for **11**, and ICy for **12**

The ^{1}H NMR spectrum of complexes **8**, **10**, and **12**, containing unsaturated NHC ligands, is characterized by a single resonance at low field for the two imidazole protons (6.50−6.80 ppm), as well as signals characteristic for their corresponding side-chain R groups. The ^{13}C NMR spectra give rise to characteristic low-field resonances for the carbeneic carbon at around 195 ppm and show one low-field signal for the three carbonyl ligands. Saturated complexes **9** and **11** result in ^{1}H NMR spectra with resonances at 3.15 and 3.59 ppm, respectively, for the ring protons of the imidazole and the expected signals for the mesityl and isopropylphenyl side chains. For these saturated NHC complexes, the ^{13}C NMR data give rise to downfield signals for the carbonyl ligands (one resonance) and one signal for the carbeneic carbon atom at significantly lower field (ca. 220 ppm) when compared to that for the unsaturated analogues. Elemental analyses for the complexes confirm their composition. To unambiguously characterize these complexes and to get a possible insight into fine structural differences between unsaturated and saturated NHCs, X-ray quality crystals were grown for $Ni(CO)_3$(IMes) (**8**), $Ni(CO)_3$(SIMes) (**9**), $Ni(CO)_3$(IPr) (**10**), $Ni(CO)_3$(SIPr) (**11**), as well as for $Ni(CO)_3$(ICy) (**12**).[10] Ball-and-stick representations are shown in Figure 2 (**8** and **9**), Figure 3 (**10** and **11**), and Figure 4 (complex **12**), and a comparison of selected bond distances and angles is provided in Table 1. All complexes show the expected tetrahedral geometry around the metal center with bond angles between 105 and 112°. For all compounds, the Ni−C(NHC) distances lie in the range of 1.96−1.98 Å, with both complexes containing the saturated NHC ligands (compounds **9** and **11**) showing slightly shorter bond distances than their corresponding analogues containing the saturated NHC ligands (1.961 Å for **9** versus 1.971 Å for **8**; 1.962 Å for **11** versus 1.979 Å for **10**). These differences are not very significant and lie within experimental error. The Ni−C(NHC) distance suggests a single-bond character, in good accordance with their exclusive σ-donor characteristics.[11] As seen for other crystallographically characterized complexes containing NHC ligands with aryl substituents, the R groups are disposed at an angle of 90° (±10) with respect to the imidazole backbone plane, resulting in a favorable steric arrangement with the metal center. In addition, the saturated imidazole backbones in the SIMes and SIPr compounds, due to the presence of two sp^3 carbons in the heterocyclic ring, show torsion angles of 6.4° (for complex **9**) and 2.6° (for complex **11**). Interestingly, this value is significantly lower than the one for free SIMes (13.4°).

Comparison of Electronic Factors Governing NHC and Phosphine Ligands. To obtain a direct comparison of the electronic factors governing NHCs with a large array of phosphine compounds of general formula $Ni(CO)_3(PR_3)$, we recorded the carbonyl stretching frequencies of complexes **8**−**12**. The values obtained are presented in Table 2 alongside those of representative $Ni(CO)_3(PR_3)$ complexes. The data clearly demonstrate that N-heterocyclic carbene ligands are better σ-donors than even the most basic phosphine, P^{t}Bu$_3$. Within the NHC ligand class, ICy (**5**) is expected to be the most basic ligand due to its alkyl-substituted nitrogen atoms (versus aryl substitution in the other ligands). Overall, the electronic differences for NHC ligands are relatively small, especially compared to the substantial electronic differences seen in phosphine ligands when moving from aryl- to alkyl-substituted

(9) Dorta, R.; Stevens, E. D.; Hoff, C. D.; Nolan, S. P. *J. Am. Chem. Soc.* **2003**, *125*, 10490−10491.

(10) Different crystal batches of **12** were measured but were disordered, and the X-ray structure determination is therefore somewhat poor ($R = 0.0978$ for data with $I > 2\sigma(I)$ and $R = 0.1169$ for all data). While important information can be obtained for its connectivity, we do not include this structure in the discussion of bond lengths and angles.

(11) (a) Herrmann, W. A.; Elison, M.; Fischer, J.; Kocher, C.; Artus, G. R. *Angew. Chem., Int. Ed.* **1995**, *34*, 2371−2374. (b) McGuinness, D. S.; Cavell, K. J.; Skelton, B. W.; White, A. H. *Organometallics* **1999**, *18*, 1596−1605.

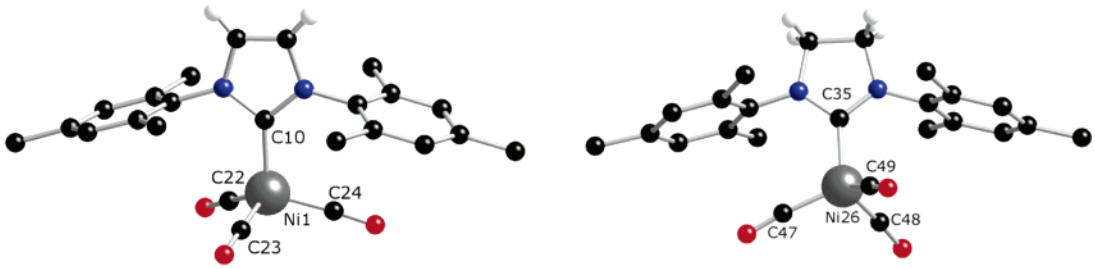

Figure 2. Ball-and-stick representation of complexes **8** (left) and **9** (right). Hydrogen atoms, except for imidazole protons, are omitted for clarity.

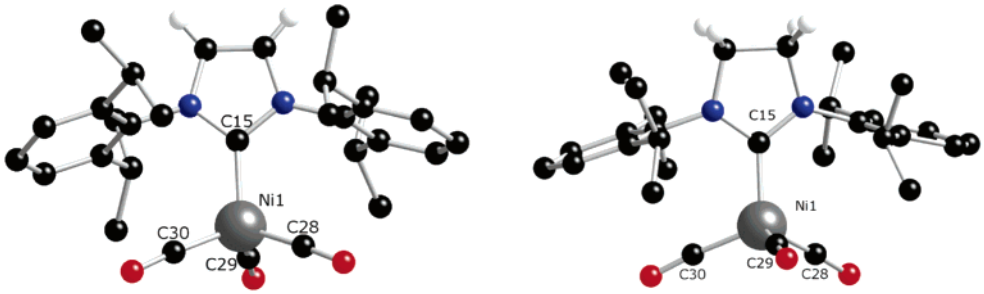

Figure 3. Ball-and-stick representation of complexes **10** (left) and **11** (right). Hydrogen atoms, except for imidazole protons, are omitted for clarity.

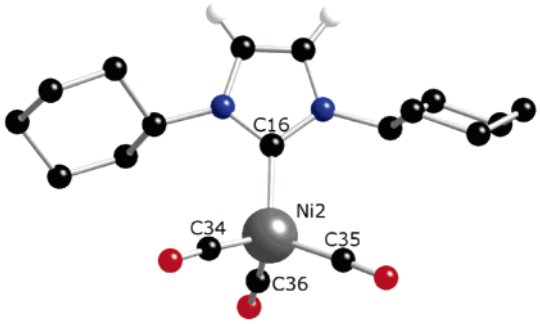

Figure 4. Ball-and-stick representation of complex **12**. Hydrogen atoms, except for imidazole protons, are omitted for clarity.

phosphorus ligands. As an example, a difference of ν_{CO} of more than 12 cm^{-1} is observed when comparing the stretching frequencies of $Ni(CO)_3(L)$ compounds for L = PPh_3 with those of the more basic, alkyl-substituted L = P^tBu_3 (Table 2). Another interesting fact is the very small difference in stretching frequency between IMes (**1**) and SIMes (**2**) in complexes **8** and **9** and IPr (**3**) and SIPr (**4**) in complexes **10** and **11**. In fact, the saturated NHC ligands are even slightly less electron-donating than their unsaturated analogues. It is worth noting that we have recently observed similar trends in the relative bond disruption enthalpies of ruthenium complexes involving the aforementioned ligands.[12] These experimental results clearly contradict the common assumption that saturated NHC ligands are more electron-donating and that metal complexes incorporating them perform better in catalysis for this reason. The recent work of Yates[13] on the relative basicity of NHC in various solvents is on note as some of the theoretical predictions fall in line with our experimental data in terms of general donor property trends of NHC but diverge in predictions of overall bonding interactions when saturated and unsaturated NHCs are concerned. Considering only ligand basicity may prove an oversimplification of the bonding picture in L_nM-NHC complexes. Our experimental data suggest that electronic factors related to the σ-donor abilities of these ligands are unlikely to play a major role in the differences in catalytic activity for unsaturated versus saturated NHCs.

Synthesis and Structure of Unsaturated $Ni(CO)_2(NHC)$ Complexes. When reacting a hexane solution containing NHC ligands IAd (**6**) and I^tBu (**7**) with a slight excess of $Ni(CO)_4$, we observed the formation of orange−red solutions. Both complexes were isolated in high yield after workup. Whereas ^1H NMR and ^{13}C NMR spectral data did not permit unequivocal structural assignment, significant infrared shifts to lower frequencies were observed, indicating a possibly different composition than $Ni(CO)_3(NHC)$ for these complexes. Indeed, elemental analysis data for the orange−red microcrystalline materials showed the composition to be in line with novel 16 electron complexes, $Ni(CO)_2(IAd)$ (**13**) and $Ni(CO)_2(I^tBu)$ (**14**) (eq 2).

$$Ni(CO)_4 + NHC \rightarrow Ni(CO)_2(NHC) + 2\ CO \qquad (2)$$

NHC = IAd for **13**, and I^tBu for **14**

Such unsaturated nickel carbonyl systems are exceedingly rare, and the only example known has been isolated as a mixture of $Ni(CO)_3(L)$ and $Ni(CO)_2(L)$ compounds.[14,15] To unambiguously confirm the molecular structure of these products, single crystals of both complexes were grown by slow evaporation of saturated diethyl ether (for **13**) and pentane (for **14**) solutions and were subjected to X-ray crystallographic analyses. Ball-and-stick diagrams of $Ni(CO)_2(IAd)$ (**13**) and $Ni(CO)_2(I^tBu)$

(12) Hillier, A. C.; Sommer, W. J.; Yong, B. S.; Peterson, J. L.; Cavallo, L.; Nolan, S. P. *Organometallics* **2003**, *22*, 4322−4326.
(13) Magill, A. M.; Cavell, K. G.; Yates, B. F. *J. Am. Chem. Soc.* **2004**, *126*, 8717−8724.
(14) Petz, W.; Weller, F.; Uddin, J.; Frenking, G. *Organometallics* **1999**, *18*, 619−626.
(15) Carbonyl-free, three-coordinate Ni(0) complexes are not uncommon; for some examples, see: (a) Wilke, G. *Angew. Chem., Int. Ed.* **1963**, *2*, 105−108. (b) Bogdanovic, B.; Kroener, M.; Wilke, G. *Justus Liebigs Ann. Chem.* **1966**, *699*, 1−23. (c) Jonas, K.; Heimbach, P.; Wilke, G. *Angew. Chem., Int. Ed.* **1968**, *7*, 949−950. (d) Gosser, L. W.; Tolman, C. A. *Inorg. Chem.* **1970**, *9*, 2350−2353. (e) Gabor, B.; Krueger, K.; Marczinke, B.; Mynott, R.; Wilke, G. *Angew. Chem., Int. Ed.* **1991**, *30*, 1666−1668. (f) Mindiola, D. J.; Hillhouse, G. L. *J. Am. Chem. Soc.* **2002**, *124*, 9976−9977.

Table 1. Selected Bond Lengths and Angles for $Ni(CO)_3$(IMes) (**8**), $Ni(CO)_3$(SIMes) (**9**), $Ni(CO)_3$(IPr) (**10**), and $Ni(CO)_3$(SIPr) (**11**)

Complex **8**		Complex **9**		Complex **10**		Complex **11**	
Ni1−C23	1.785(4)	Ni26−C49	1.7706	Ni1−C29	1.783(3)	Ni1−C29	1.771(5)
Ni1−C22	1.797(4)	Ni26−C48	1.7807	Ni1−C28	1.796(2)	Ni1−C28	1.787(4)
Ni1−C24	1.801(3)	Ni26−C47	1.7916	Ni1−C30	1.801(3)	Ni1−C30	1.810(4)
Ni1−C10	1.971(3)	Ni26−C35	1.9602	Ni1−C15	1.979(2)	Ni1−C15	1.962(4)
C23−Ni1−C22	109.76(15)	C49−Ni26−C48	108.3	C29−Ni1−C28	109.01(11)	C29−Ni1−C28	109.30(19)
C23−Ni1−C24	109.89(16)	C49−Ni26−C47	111.1	C29−Ni1−C30	109.59(11)	C29−Ni1−C30	106.25(17)
C22−Ni1−C24	111.46(16)	C48−Ni26−C47	107.4	C28−Ni1−C30	111.46(10)	C28−Ni1−C30	111.63(18)
C23−Ni1−C10	108.46(14)	C49−Ni26−C35	108.3	C29−Ni1−C15	105.34(9)	C29−Ni1−C15	108.01(17)
C22−Ni1−C10	107.99(14)	C48−Ni26−C35	110.8	C28−Ni1−C15	111.03(9)	C28−Ni1−C15	111.79(17)
C24−Ni1−C10	109.22(14)	C47−Ni26−C35	111.0	C30−Ni1−C15	110.22(9)	C30−Ni1−C15	109.66(16)

Table 2. IR Values for the Carbonyl Stretching Frequencies in $Ni(CO)_3(L)$ and $Ni(CO)_2(L)$ Complexes

ligand	complex	ν_{CO} (A_1); CH_2Cl_2	ν_{CO} (E); CH_2Cl_2	ν_{CO} (A_1); hexane	ν_{CO} (E); hexane
IMes (**1**)	$Ni(CO)_3$(IMes) (**8**)	2050.7	1969.8	2054.0	1978.2, 1971.0
SIMes (**2**)	$Ni(CO)_3$(SIMes) (**9**)	2051.5	1970.6	2054.7	1980.0, 1972.3
IPr (**3**)	$Ni(CO)_3$(IPr) (**10**)	2051.5	1970.0	2055.1	1980.4, 1972.3
SIPr (**4**)	$Ni(CO)_3$(SIPr) (**11**)	2052.2	1971.3	2056.0	1982.6, 1973.7
ICy (**5**)	$Ni(CO)_3$(ICy) (**12**)	2049.6	1964.6	2052.4	1973.4, 1968.0
IAd (**6**)	$Ni(CO)_2$(IAd) (**13**)			2007.2	1926.3
I^{t}Bu (**7**)	$Ni(CO)_2$(I^{t}Bu) (**14**)			2009.7	1928.6
P^tBu_3[a]	$Ni(CO)_3(P^tBu_3)$	2056.1	1971		
PCy_3[a]	$Ni(CO)_3(PCy_3)$	2056.4	1973		
PPh_3[a]	$Ni(CO)_3(PPh_3)$	2068.9	1990		

[a] From ref 8.

(**14**), alongside selected bond lengths and angles, are presented in Figures 5 (for **13**) and 6 (for **14**). Both complexes show only slightly distorted trigonal structures with angles between 117 and 123°. The Ni−C(NHC) bond distances of 1.953(2) (**13**) and 1.957(1) Å (**14**) are marginally shorter than those in the saturated complexes **8**−**12**, but significantly longer than for those of the crystallographically characterized, homoleptic $Ni(IMes)_2$ compound, which shows bond lengths of 1.827 and 1.830 Å.[16] One of the carbon atoms from both side-chain R groups in **13** and **14** is approaching the metal center. Although these Ni···C(R) distances lie outside the range seen for agostic interactions with first-row metal centers (Ni···C(R) ≥ 3 Å),[17] the structures give an explanation for the higher steric requirements of I^{t}Bu (**6**) and IAd (**7**). In fact, these two ligands are the only ones in the series to contain α-carbon atoms in the side chains that are bound to three additional C atoms. Whereas the aromatic IMes (**1**), SIMes (**2**), IPr (**3**), and SIPr (**4**), as well as ICy (**5**), can orient their R groups perpendicularly to the imidazole plane and therefore minimize steric interactions with the metal center, such an arrangement cannot be reached for IAd (**6**) and I^{t}Bu (**7**).

Experimental Determination of Ni−C(NHC) Bond Dissociation Enthalpies (BDE). This work began as an attempt to spectroscopically detect the saturated tricarbonyl adducts of the I^{t}Bu and IAd compounds under CO pressure, illustrated for $Ni(CO)_2$(IAd) in eq 3 below:

$$Ni(CO)_2(IAd) + CO \rightleftharpoons Ni(CO)_3(IAd) \qquad (3)$$

Instead of observing the equilibrium associated with eq 3, net displacement of either I^{t}Bu or IAd by 2 mol of CO occurred

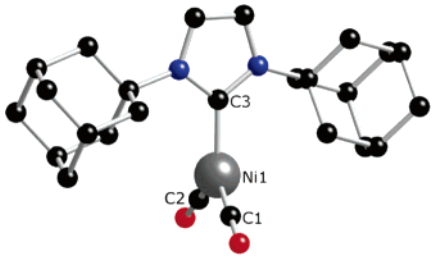

Figure 5. Ball-and-stick representation of complex **13**. Hydrogen atoms are omitted for clarity. Selected bond lengths (Å) and angles (deg): Ni1−C1 1.7583(19), Ni1−C2 1.761(2), Ni1−C3 1.9528(16); C1−Ni1−C2 123.01(10), C1−Ni1−C3 116.91(9), C2−Ni1−C3 119.93(10).

according to eq 4. Variable temperature spectroscopic data for eq 4 are shown in Figure 7.

$$Ni(CO)_2(NHC) + 2\ CO \rightleftharpoons Ni(CO)_4 + NHC \qquad (4)$$

$$NHC = IAd \text{ or } I^tBu$$

Although eq 4 is most readily approached through the intermediate $Ni(CO)_3(NHC)$, no spectroscopic sign of this intermediate could be found for complexes of either IAd or I^{t}Bu. This implies that $Ni(CO)_3(NHC)$ under CO has only a fleeting existence for IAd and I^{t}Bu, and that the NHC ligands are readily displaced by CO to form $Ni(CO)_4$.

In contrast, the stable complexes, $Ni(CO)_3$(IMes) and $Ni(CO)_3$(SIMes), are not carbonylated to $Ni(CO)_4$ even under pressure of CO (eq 5). Spectroscopic data under argon and under pressure of CO [550 psi CO for (**9**) and 350 psi CO for (**8**)] are shown in Figure 8.

$$Ni(CO)_3(NHC) + CO \not\longrightarrow Ni(CO)_4 + NHC \qquad (5)$$

$$NHC = IMes, SIMes$$

The complexes are essentially unchanged under these conditions. Solutions left under pressure overnight show no sign of

(16) Arduengo, A. J., III; Gamper, S. F.; Calabrese, J. C.; Davidson, F. *J. Am. Chem. Soc.* **1994**, *116*, 4391−4394.
(17) (a) Brookhart, M.; Green, M. L. H.; Wong, L. *Prog. Inorg. Chem.* **1988**, *36*, 1−124. (b) Crabtree, R. H. *Angew. Chem., Int. Ed.* **1993**, *32*, 789−805.

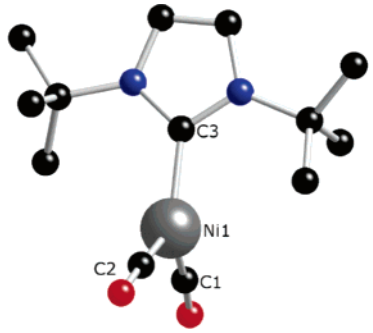

Figure 6. Ball-and-stick representation of complex **14**. Hydrogen atoms, except for imidazole protons, are omitted for clarity. Selected bond lengths (Å) and angles (deg): Ni1−C1 1.7489(13), Ni1−C2 1.7535(13), Ni1−C3 1.9569(11); C1−Ni1−C2 120.10(6), C1−Ni1−C3 117.25(5), C2−Ni1−C3 122.36(5).

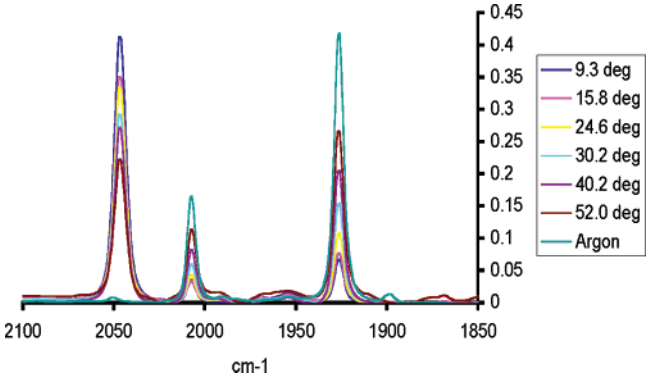

Figure 7. Variable temperature FT-IR spectral data for $Ni(CO)_4 + IAd \rightarrow Ni(CO)_2(IAd) + 2\ CO$. The band near 2046 cm^{-1} is due to $Ni(CO)_4$ and increases with decreasing temperature.

$Ni(CO)_4$ with its characteristic band at 2046 cm^{-1}. In contrast, $Ni(CO)_2(IAd)$ and $Ni(CO)_2(I^tBu)$ are rapidly and quantitatively converted to $Ni(CO)_4$ under pressure of CO.

These observations allow some bracketing of the Ni−C(NHC) bond strength in the tricarbonyl $Ni(CO)_3$(IMes) complex and the unstable proposed intermediate, $Ni(CO)_3$(IAd). The most recent gas-phase data for sequential Ni−CO bond strengths[18] are summarized in eq 6 (numbers are in kcal/mol):

$$Ni(CO)_4 \xrightarrow{24} CO + Ni(CO)_3 \xrightarrow{28} CO + Ni(CO)_2 \xrightarrow{47} CO + Ni(CO) \xrightarrow{41} CO + Ni \quad (6)$$

The sum of the gas-phase bond strengths in $Ni(CO)_4$ of 141.8 kcal/mol is based on combustion calorimetric measurements.[19] This value leads to an average Ni−CO bond dissociation energy of ≈35 kcal/mol. There is more individual error in the partitioning of these bond strengths than there is in the average, but it is the initial first two dissociations that are most important in the current system.

Using the value in eq 6 for the first bond dissociation energy of $Ni(CO)_4$ can provide qualitative insight into the magnitude of the Ni−C(NHC) bond strength in $Ni(CO)_3$(NHC) complexes. The observation that $Ni(CO)_3$(IMes) resists carbonylation under CO pressure and that no evidence can be found for $Ni(CO)_3$(IAd) clearly implies that the $(CO)_3$**Ni**−**C**(IMes) ≥ 24 ≥ (IAd)-**C**−**Ni**$(CO)_3$. It should be pointed out that previous calorimetric studies have shown that the enthalpy of binding for IMes compared to that for IAd in both metals,[20] and sulfur,[21] is more exothermic in the order of 10 kcal/mol. That trend is in keeping with the qualitative observation for the nickel tricarbonyl complexes, as well. Furthermore, these qualitative observations are supported by theoretical calculations discussed later.

The sum of the first two bond dissociation energies for $Ni(CO)_4$ (52 kcal/mol) can be combined with variable temperature equilibrium data for the formation of $Ni(CO)_2$(NHC) (approaching the equilibrium in eq 4 from the right) to generate absolute estimates for the Ni−C(NHC) bond strength in the dicarbonyl complexes. Plots of ln K_{eq} versus $1/T$ for formation of $Ni(CO)_2$(NHC) are shown in Figure 9 and lead to derived thermodynamic data for the formation of $Ni(CO)_2$(IAd) [$\Delta H = 10.2 \pm 0.3$ kcal/mol and $\Delta S = 41 \pm 3$ cal/mol deg] and for the formation of $Ni(CO)_2(I^tBu)$ [$\Delta H = 14.6 \pm 0.4$ kcal/mol and $\Delta S = 53 \pm 5$ cal/mol deg].

These data lead directly to estimates of the Ni−C(NHC) bond strength in these dicarbonyls of 42 [for Ni−C(IAd)] and 37 kcal/mol [for Ni−C(I^tBu)]. The positive entropies of reaction are in keeping with the release of 2 mol of CO upon uptake of the carbene. The less positive value for binding of IAd compared to that of I^tBu may be due to a relatively greater loss of rotational freedom in binding of IAd. Thus, the greater enthalpic preference for binding of IAd is partially negated by a corresponding less favorable entropy of binding.

In view of the fact that both I^tBu and IAd were in equilibrium with $Ni(CO)_4$, reaction 7 was investigated.

$$Ni(CO)_2(I^tBu) + IAd \rightleftharpoons Ni(CO)_2(IAd) + I^tBu \quad (7)$$

In principle, since both carbene complexes establish an equilibrium through intermediary $Ni(CO)_4$, direct measurement of eq 7 was deemed possible. In practice, even under argon atmosphere with no sign of intermediate $Ni(CO)_4$, eq 7 is established within minutes at room temperature. The reaction depicted in eq 7 can be approached from either side and yields an estimate of $K_{eq} \cong 5$ at 20 °C, in good agreement with comparative data calculated from data in Figure 9.

The relatively rapid establishment of the equilibrium in eq 7 for the carbene exchange as well as the absence of detectable $Ni(CO)_4$ implies that an associative exchange as shown in eq 8 may be operative.

$$Ni(CO)_2(I^tBu) + IAd \rightleftharpoons Ni(CO)_2(I^tBu)(IAd) \rightleftharpoons Ni(CO)_2(IAd) + I^tBu \quad (8)$$

Thus, despite severe steric crowding in a complex, such as $Ni(CO)_2(I^tBu)$(IAd), the unsaturated $Ni(CO)_2$(NHC) compounds seem to be capable of undergoing associative exchange reactions. This reactivity pattern might also be operative in the interaction of $Ni(CO)_2$(NHC) compounds with olefins (see discussion below).

Steric Requirements of NHCs: Molecular Modeling Studies for $Ni(CO)_2$(NHC) versus $Ni(CO)_3$(NHC). The striking difference in reactivity of NHC ligands IAd and I^tBu toward

(18) Data taken from: Sunderlin, L. S.; Wang, D.; Squires, R. R. *J. Am. Chem. Soc.* **1992**, *114*, 2788−2796.
(19) Fischer, A. K.; Cotton, F. A.; Wilkinson, G. *J. Am. Chem. Soc.* **1957**, *79*, 2044−2046.
(20) Huang, J.; Schanz, H.-J.; Stevens, E. D.; Nolan, S. P. *Organometallics* **1999**, *18*, 2370−2375.
(21) Huang, J.; Schanz, H.-J.; Nolan, S. P.; Capps, K. B.; Bauer, A.; Hoff, C. D. *Inorg. Chem.* **2000**, *38*, 1042−1045.

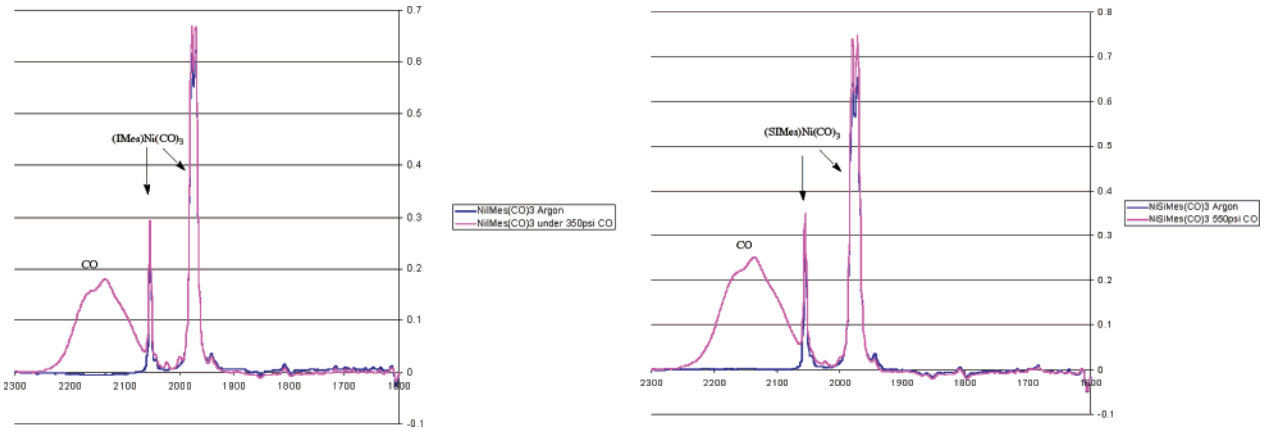

Figure 8. High-pressure FT-IR experiments of $Ni(CO)_3$(IMes) (**8**, left) and $Ni(CO)_3$(SIMes) (**9**, right) with CO.

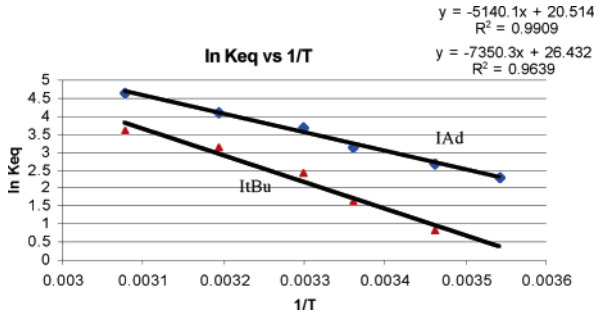

Figure 9. Van't Hoff plots for $Ni(CO)_2$(IAd) (**13**, above) and $Ni(CO)_2(I^tBu)$ (**14**, below).

$Ni(CO)_4$, producing unsaturated dicarbonyl complexes, seems to be based on higher steric requirements of these two ligands.[22] To rationalize the experimental data, and to possibly afford a direct steric comparison between NHCs and phosphine ligands, di- and tricarbonyl nickel complexes were investigated by DFT calculations. Geometries and energies of the $Ni(CO)_2$(NHC) and $Ni(CO)_3$(NHC) structures were optimized for R = I^tBu, SI^tBu, IAd, IMes, SIMes, IPr, SIPr, and ICy (both with full QM and with QM/MM techniques). For the phosphine-based systems, full QM geometry optimizations were performed for the $Ni(CO)_2(PR_3)$ and $Ni(CO)_3(PR_3)$ structures, with R = H, Ph, Cy, and ^{t}Bu. The calculated BDE values of CO and L in $Ni(CO)_3$(L) and $Ni(CO)_2$(L) systems (L = NHC or PR_3) are reported in Table 3.

The calculated BDE values indicate that CO is weakly bound to the I^tBu-, SI^tBu-, and IAd-based complexes (BDE ≈ 10 kcal/mol), whereas CO is much more strongly bound to the IPr, SIPr, ICy, IMes, and SIMes complexes (BDE > 25 kcal/mol). These results are in good qualitative agreement with the experimental fact that $Ni(CO)_2$(NHC) complexes are observed for NHC = IAd and I^tBu, while $Ni(CO)_3$(NHC) complexes are observed for the other NHC ligands. The BDEs calculated for the NHC ligands show a similar trend since the BDEs of the NHC ligand in the I^tBu-, SI^tBu-, and IAd-based $Ni(CO)_3$(NHC) complexes are roughly 20 kcal/mol lower than that in the IMes, SIMes, IPr, SIPr, and ICy complexes. The BDEs calculated for the NHC ligand in the $Ni(CO)_2$(IAd) and $Ni(CO)_2(I^tBu)$ complexes (46.5 and 44.3 kcal/mol, respectively) are in excellent agreement with the experimental values (43 ± 3 and 39 ± 3 kcal/mol, respectively).

To rationalize the different behavior shown by the two groups of NHC-based complexes, we calculated the BDE of CO in the $Ni(CO)_3$(NHC) systems with a combined QM/MM approach. Within this approach, all the unsaturated (IAd, I^tBu, ICy, IPr, and IMes) and saturated (SI^tBu, SIPr, and SIMes) NHC ligands share the same QM part (see the Computational Details), and different behavior can be related to their different steric properties. The numbers in Table 3 indicate that the QM/MM approach substantially replicates the full QM calculations. Since the QM/MM BDEs are very close to QM values, the difference between the two groups of NHC ligands can be attributed to steric factors exclusively.

Table 3. CO and L BDE Values (in kcal/mol) in the $Ni(CO)_2$(L) and $Ni(CO)_3$(L) Complexes (L = NHC ligand or phosphine) and Calculated $\%V_{bur}$ of the Free NHC and PR_3 Ligands

ligand	BDE of CO in $Ni(CO)_3$(L)	BDE of L in $Ni(CO)_3$(L)	BDE of L in $Ni(CO)_2$(L)	$\%V_{bur}$
I^tBu	13.3 (15.6)[a]	24.0	44.3	37
SI^tBu	10.3 (13.1)[a]	21.8	45.1	38
IAd	7.6 (14.1)[a]	20.4	46.5	37
IMes	28.3 (27.2)[a]	41.1	46.5	26
SIMes	26.8 (26.4)[a]	40.2	47.2	27
IPr	26.7 (27.2)[a]	38.5	45.4	29
SIPr	25.6 (25.8)[a]	38.0	46.1	30
ICy	27.0 (26.1)[a]	39.6	46.3	23
PH_3	30.7	22.7	25.7	17
PPh_3	30.4	26.7	30.0	22
PCy_3				26
P^tBu_3	27.4	28.0	34.3	30

[a] Values in parentheses were obtained with the QM/MM technique.

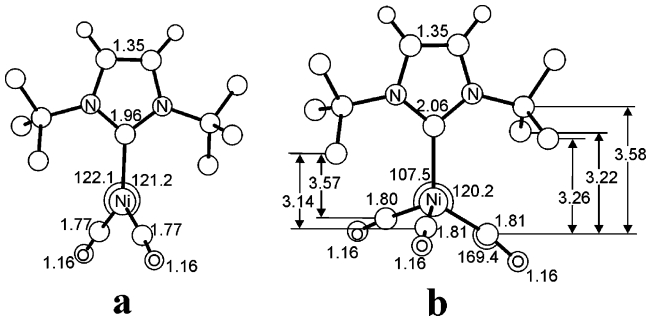

Figure 10. Bond distances and angles for unsaturated (a) and saturated (b) complexes with I^tBu.

(22) The concept of "steric pressure" noted by Power and others in the use of *m*-terphenyl ligands (isosteric with some NHC presented here) should be brought to the reader's attention. Similar steric pressures, as the one described here for IAd and I^tBu, lead to the stabilization and formation of monomeric versus dimeric or dimeric versus trimeric architectures in main-group-*m*-terphenyl compounds. For example, see: Hino, S.; Olmstead, M.; Phillips, A. D.; Wright, R. J.; Power, P. P. *Inorg. Chem.* **2004**, *43*, 7346−7352 and references cited therein.

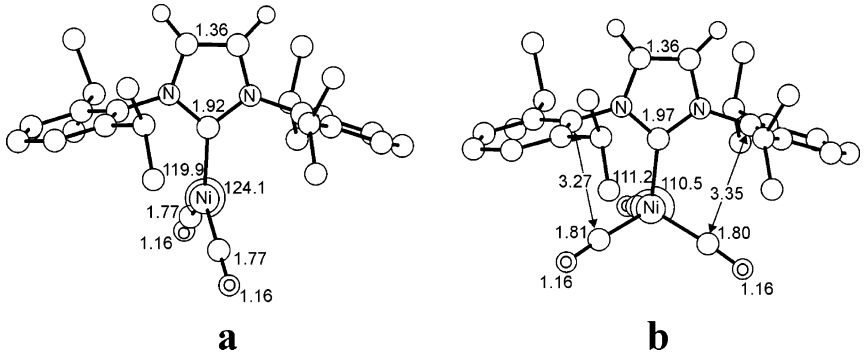

Figure 11. Bond distances and angles for unsaturated (a) and saturated (b) complexes with IPr.

To quantify the steric factors characterizing these ligands, we measured the amount of volume of a sphere centered on the metal, buried by overlap with atoms of the various NHC and phosphine ligands, $\%V_{bur}$. The volume of this sphere would represent the space around the metal atom that must be shared by the different ligands upon coordination. Of course, the bulkier a specific ligand, the larger the amount of that sphere will be occupied by the ligand, that is, greater $\%V_{bur}$. To have an aseptic estimate of the bulkiness of the various ligands, we examined the DFT optimized geometries of the free ligands and positioned the putative metal atom 2 Å from the coordinating C atom for the NHC ligand class and 2.28 Å from the coordinating P atom for the PR_3 ligands.[23] The radius of the sphere was chosen to be 3 Å. A compilation of $\%V_{bur}$ values is presented in Table 3. The larger values of $\%V_{bur}$ of the I^{t}Bu, SI^{t}Bu, and IAd ligands, relative to the IMes, SIMes, IPr, SIPr, and ICy ligands, are in qualitative agreement with the different BDEs we calculated for the two groups of NHC ligands.

Geometrical inspection of the calculated structures for the exemplary cases, $Ni(CO)_2(I^tBu)$ and $Ni(CO)_3(I^tBu)$, supports the previous findings. As reported in Figure 10, $Ni(CO)_3(I^tBu)$ shows several steric interactions, indicated by short distances, between the *tert*-butyl group and the CO molecules, relative to $Ni(CO)_2(I^tBu)$. These strong steric interactions in $Ni(CO)_3(I^t$-Bu) result in the severe distortion of one of the Ni−C−O angles from the ideal value of 180° to assume a value of 169.4°. In contrast, $Ni(CO)_3$(IPr) is characterized by very few short distances between the NHC ligand and the CO molecules, which explains its stability (Figure 11). Incidentally, the calculated geometries are in an overall good agreement with the corresponding X-ray structures.

With regard to a comparison between NHC- and PR_3-based systems, we note that the CO BDE values in the PR_3 systems of Table 3 are quite similar, although the group R of PR_3 goes from extremely small, for R = H, to extremely bulky, for R = ^{t}Bu. This clearly indicates that steric effects play almost no role in determining the stability of the $Ni(CO)_3(PR_3)$ systems. Moreover, the BDEs of the CO in the PR_3 systems and in the less bulky NHC systems are similar, which suggests a high stability of the PR_3-based tricarbonyl systems. The BDEs we calculated for the NHC ligands are remarkably higher than the BDEs we calculated for the PR_3 ligands, a finding that is in agreement with the common assumption that NHC ligands bind more tightly to LTMs than phosphines.

Most importantly, calculation of the $\%V_{bur}$ of the PR_3 systems allows a direct comparison of the steric requirements of the NHC and phosphine ligand families. The calculated values for $\%V_{bur}$ show that sterically, the very bulky phosphine ligand, P^{t}Bu$_3$, is best compared to IPr and SIPr; PCy_3 gives a $\%V_{bur}$ value close to the ones found for IMes and SIMes, whereas PPh_3 has a $\%V_{bur}$ similar to that for ICy. Incidentally, the steric requirements for tertiary phosphines and NHCs we find here coincide with catalytic data in the literature. For example, it has been shown that for palladium-catalyzed coupling reactions of aryl chlorides, where 12-electron L−Pd(0) compounds are involved, bulky ligands, such as P^{t}Bu$_3$ and IPr/SIPr, outperform PCy_3 and IMes/SIMes.[6,24] On the other hand, in ruthenium-catalyzed metathesis reactions, where the active catalyst is thought to involve a (L)-$RuCl_2$(=CR_2) species, the ligands performing best are PCy_3 and SIMes/IMes, with more bulky phosphine and NHC ligands being considerably less active.[3d−g] Sterically most demanding ligands, I^{t}Bu, SI^{t}Bu, and IAd, are all significantly more bulky than P^{t}Bu$_3$, a fact that in turn might lead to different behavior in reactivity and catalysis of metals incorporating these ligands.[25]

Reactivity of $Ni(CO)_n$(NHC) Complexes. Reactivity toward substitution of the carbonyl ligands in the $Ni(CO)_n$(NHC) (n = 2 or 3) complexes was also investigated by exploring their interaction with different olefins. The results obtained for the saturated $Ni(CO)_3$(NHC) systems were not surprising, showing that these complexes are essentially inert toward CO substitution at room temperature with the substrates used (see below). The unsaturated $Ni(CO)_2$(NHC) compounds **13** and **14** did also not react with olefins, such as styrene and tetracyanoethylene. In contrast, $Ni(CO)_2(I^tBu)$ (**14**) reacted readily with the small and electron-poor trifluoropropene. When an orange−red pentane solution of $Ni(CO)_2(I^tBu)$ (**14**) was saturated with $C_3F_3H_3$ (excess), an immediate color change to bright yellow was observed with concomitant release of CO. Workup yielded the unsaturated, monocarbonyl complex $Ni(CO)(C_3H_3F_3)(I^tBu)$ (**15**) selectively and in high yield. The complex arising from double substitution of CO, $Ni(C_3H_3F_3)_2(I^tBu)$ (eq 9), was not formed. The carbonyl stretching frequency of **15** is found at 1982 cm^{-1}. ^{1}H, ^{13}C, and ^{19}F NMR spectra are consistent with its formulation,

(23) This value reflects the bond distances found in crystallographically characterized complexes of this type: (a) Pickardt, J.; Rosch, L.; Schumann, H. *Z. Anorg. Allg. Chem.* **1976**, *426*, 66−76. (b) Baumgartner, T.; Moors, P.; Nieger, M.; Niecka, E. *Organometallics* **2002**, *21*, 4919−4926. (c) Gudat, D.; Bajorat, V.; Hap, S.; Niegler, M.; Schroder, G. *Eur. J. Inorg. Chem.* **1999**, 1169−1174.

(24) For a recent review on the use of P^{t}Bu$_3$ in these transformations, see: Littke, A. F.; Fu, G. C. *Angew. Chem., Int. Ed.* **2002**, *41*, 4176−4211.

(25) We have very recently taken advantage of these findings in a Rh−NHC system: Dorta, R.; Stevens, E. D.; Nolan, S. P. *J. Am. Chem. Soc.* **2004**, *126*, 5054−5055.

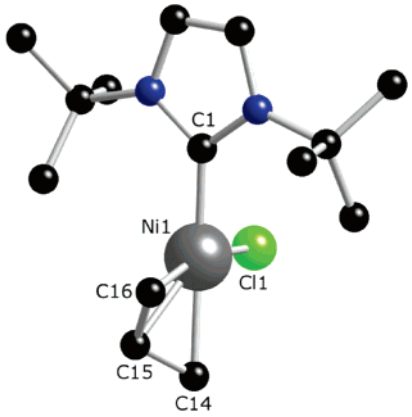

Figure 12. Ball-and-stick representation of complex **16**. Hydrogen atoms omitted for clarity. Selected bond lengths (Å) and angles (deg): Ni1−C1 1.926(2), Ni1−C15 1.981(3), Ni1−C16 1.993(2), Ni1−C14 2.058(3), Ni1−Cl1 2.2322(7); C1−Ni1−C15 132.46(11), C1−Ni1−C16 95.92(11), C15−Ni1−C16 41.06(12), C1−Ni1−C14 167.35(12), C15−Ni1−C14 39.48(12), C16−Ni1−C14 72.60(12), C1−Ni1−Cl1 97.88(7), C15−Ni1−Cl1 126.75(9), C16−Ni1−Cl1 166.04(9), C14−Ni1−Cl1 93.46(9).

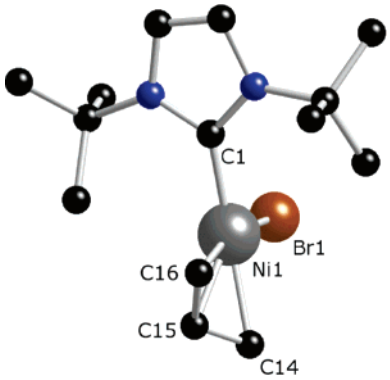

Figure 13. Ball-and-stick representation of complex **17**. Hydrogen atoms omitted for clarity. Selected bond lengths (Å) and angles (deg): Br1−Ni1 2.3970(8), Ni1−C1 1.957(4), Ni1−C15 1.987(5), Ni1−C16 2.021(5), Ni1−C14 2.096(5); C1−Ni1−C15 132.8(2), C1−Ni1−C16 95.8(2), C15−Ni1−C16 41.3(3), C1−Ni1−C14 167.4(2), C15−Ni1−C14 38.3(3), C16−Ni1−C14 72.4(3), C1−Ni1−Br1 97.61(11), C15−Ni1−Br1 126.76(19), C16−Ni1−Br1 166.49(17), C14−Ni1−Br1 94.2(2).

and elemental analysis confirmed the composition of Ni(CO)-($C_3H_3F_3$)(I^tBu) (**15**).

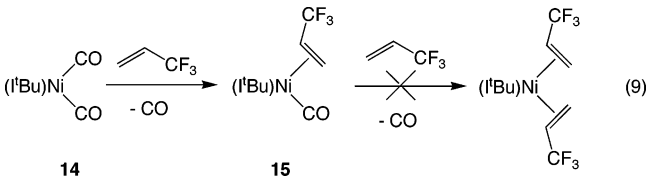

Substitution of both CO ligands is achieved when the unsaturated compounds **13** and **14** are reacted with a slight excess of allyl chloride or allyl bromide. In fact, these substrates add readily to these complexes, giving the allyl halide Ni(II) complexes **16**−**19** in quantitative yield via oxidative addition of the allyl halides. NiCl(C_3H_5)(I^tBu) (**16**), NiBr(C_3H_5)(I^tBu) (**17**), NiCl(C_3H_5)(IAd) (**18**), and NiBr(C_3H_5)(IAd) (**19**) were synthesized according to eq 10 and were fully characterized by NMR spectroscopy and elemental analysis. In addition, crystals suitable for an X-ray diffraction analysis for complexes **16** and **17** were grown by slow evaporation of concentrated acetone solutions. Ball-and-stick views of these complexes, including relevant bond lengths and angles, are found in Figures 12 (for **16**) and 13 (for **17**). In both cases, distorted square-planar coordinations around the nickel center are observed. The halide anions are located cis to the carbene ligand, and the allyl moiety is η^3-coordinated to the nickel with one terminal carbon trans to the carbene and the second terminal carbon trans to the halide ligand. In both complexes, the Ni−C_{allyl} bonds opposite the NHC moiety are elongated as a result of a strong trans effect of the NHC ligand. Finally, the Ni−C(NHC) bonds are somewhat shorter than those for the Ni(0) complexes described above.

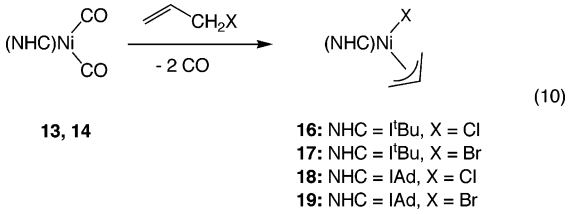

Conclusions

To gain insight into electronic and steric factors governing NHC ligands and to compare them with the widely used phosphine ligand class, we have performed a detailed experimental and computational study on the interaction of the most commonly used monodentate NHC ligands with $Ni(CO)_4$. In most of the cases, saturated $Ni(CO)_3$(NHC) were obtained. IR carbonyl stretching frequencies clearly showed that NHCs are better electron donors than the most basic tertiary phosphines. Within the NHC ligand class, saturated NHC ligands are not better donors than their unsaturated analogues and alkyl-substituted NHCs are only marginally more electron-donating than their aryl-substituted counterparts. Reaction of IAd and I^tBu with $Ni(CO)_4$ gave rise to unsaturated $Ni(CO)_2$(NHC) compounds, indicating that both these ligands are substantially more bulky than P^tBu_3. Due to the unsaturated nature of these $Ni(CO)_2$(NHC) complexes, both the NHC and the carbonyl ligands could be displaced. Reacting $Ni(CO)_2$(NHC) with CO afforded the starting $Ni(CO)_4$ complex quantitatively and allowed for the determination of Ni−C(NHC) bond dissociation energies. Substitution of one carbonyl ligand was observed when reacting $Ni(CO)_2$(NHC) with trifluoropropene and yielded the unsaturated Ni(CO)($C_3H_3F_3$)(NHC) compound selectively. Both CO ligands were displaced when $Ni(CO)_2$(NHC) was treated with either allyl chloride or allyl bromide. The resulting allyl halide complexes of general formula Ni$X(C_3H_5)$(NHC) were obtained through oxidative addition of these substrates.

To shed light on the experimental results, we performed DFT calculations on a series of $Ni(CO)_2$(L) and $Ni(CO)_3$(L) compounds (L = NHC or PR_3). In line with experimental results, the calculations showed that both $Ni(CO)_3$(IAd) and $Ni(CO)_3$-(I^tBu) are inherently unstable, as seen in the BDE values for both the CO and NHC ligands. Furthermore, the Ni−PR_3 BDE values obtained are generally lower than those for Ni−NHC, in agreement with the common assumption that NHC ligands bind more tightly to LTMs. Most importantly, we have established a method to quantify the steric factors characterizing NHCs and phosphines, enabling a direct comparison between these ligand classes. The values for the different ligands are measured as $\%V_{bur}$. All values obtained are in excellent

agreement with experimental data and show that IAd and I^{t}Bu are substantially more bulky than P^{t}Bu$_3$ and other NHC ligands.

Experimental Section

General Considerations. All reactions were carried out using standard Schlenk techniques under an atmosphere of dry argon or in MBraun gloveboxes containing dry argon and less than 1 ppm oxygen. Solvents were distilled from appropriate drying agents or were passed through an alumina column in an MBraun solvent purification system. Other anhydrous solvents were purchased from Aldrich and degassed prior to use by purging with dry argon and were kept over molecular sieves. Solvents for NMR spectroscopy were degassed with argon and dried over molecular sieves. NMR spectra were collected on a 400 MHz Varian Gemini spectrometer. Infrared spectra were recorded on a PE 2000 FT-IR spectrometer. Elemental analyses were performed by Desert Analytics, Tucson, AZ, and by Robertson Microlit Labs. Carbene ligands **1**−**7** were synthesized following literature procedures.[26] Ni(CO)$_4$ was graciously supplied by Dupont CR&D. Special care has been taken while manipulating the *EXTREMELY TOXIC* Ni(CO)$_4$. All manipulations have been carried out in the glovebox, using additional protective gloves. Ni(CO)$_4$ was constantly maintained at −50 °C. The solutions containing the NHC ligands were cooled to −50 °C, and Ni(CO)$_4$ was added via syringe at the same temperature. The slight excess of Ni(CO)$_4$ at the end of each reaction (carried out in Schlenk glassware inside the glovebox) was evaporated and trapped into a toluene solution containing phosphines.

Synthesis of Ni(CO)$_3$(IMes) (8). A hexane solution (20 mL) of IMes (1000 mg, 3.290 mmol) was added dropwise to a hexane solution (4 mL) of Ni(CO)$_4$ (674 mg, 3.948 mmol). Evolution of CO was observed with concomitant formation of a partial off-white precipitate. The pale suspension was stirred at room temperature for 1 h, and the volatiles were removed in vacuo. The solid was collected, washed with cold pentane (−50 °C, 2 × 5 mL), and dried in vacuo to give complex **8** as a beige solid. Crystals were obtained by slow evaporation of a saturated pentane solution. Yield: 1397 mg (95%). Anal. Calcd for $C_{24}H_{24}N_2NiO_3$ (MW 447.15): C, 64.46; H, 5.41; N, 6.26. Found: C, 64.06; H, 5.58; N, 5.86. ^{1}H NMR (C_6D_6, 400 MHz, δ): 6.81 (s, 4H, IMes−C**H**−Ar), 6.25 (s, 2H, NC**H**=C**H**N), 2.12 (s, 6H, IMes−C**H**$_3$), 2.02 (s, 12H, IMes−C**H**$_3$). ^{13}C NMR (C_6D_6, 100.6 MHz, δ): 198.73 (s, N−**C**−N), 194.30 (s, **C**O), 139.22 (s, IMes−**C**), 138.15 (s, IMes−**C**), 135.76 (s, IMes−**C**), 129.75 (s, IMes−**C**), 122.13 (s, N**C**H=**C**HN), 21.39 (s, IMes−**C**H$_3$), 17.93 (s, IMes−**C**H$_3$). IR ν_{CO} (hexane, cm^{-1}): 2054.0 (s), 1978.2 (vs), 1971.0 (vs). IR ν_{CO} (CH_2Cl_2, cm^{-1}): 2050.7 (s), 1969.8 (vs).

Synthesis of Ni(CO)$_3$(SIMes) (9). Addition of a hexane solution (3 mL) containing SIMes (300 mg, 0.980 mmol) to a hexane solution (3 mL) of Ni(CO)$_4$ (198 mg, 1.159 mmol) under stirring led to the evolution of CO. The transparent solution was stirred at room temperature for 2 h, resulting in partial precipitation of a white solid. Subsequently, the volatiles were removed in vacuo, yielding a white solid, and the compound was washed with cold pentane (−50 °C, 2 × 3 mL), affording complex **9** as a white powder. X-ray quality crystals were obtained from a saturated hexane solution. Yield: 400 mg (91%). Anal. Calcd for $C_{24}H_{26}N_2NiO_3$ (MW 449.17): C, 64.18; H, 5.83; N, 6.24. Found: C, 63.97; H, 5.70; N, 6.06. ^{1}H NMR (C_6D_6, 400 MHz, δ): 6.87 (s, 4H, SIMes−C**H**−Ar), 3.15 (s, 4H, NC**H**$_2$−C**H**$_2$N), 2.20 (s, 12H, SIMes−C**H**$_3$), 2.12 (s, 6H, SIMes−C**H**$_3$). ^{13}C NMR (C_6D_6, 100.6 MHz, δ): 220.40 (s, N−**C**−N), 198.73 (s, **C**O), 138.54 (s, SIMes−**C**), 138.35 (s, SIMes−**C**), 136.67 (s, SIMes−**C**), 130.17 (s, SIMes−**C**), 50.67 (s, N**C**H$_2$**C**H$_2$N), 21.38 (s, SIMes−**C**H$_3$), 18.02 (s, SIMes−**C**H$_3$). IR ν_{CO} (hexane, cm^{-1}): 2054.7 (s), 1980.0 (vs), 1972.3 (vs). IR ν_{CO} (CH_2Cl_2, cm^{-1}): 2051.5 (s), 1970.6 (vs).

Synthesis of Ni(CO)$_3$(IPr) (10). A THF solution (5 mL) of Ni(CO)$_4$ (143 mg, 0.84 mmol) was added to a stirred THF solution (5 mL) containing IPr (271 mg, 0.70 mmol). The resulting pale yellow solution was left stirring at room temperature for 2 h, and then the volatiles were removed in vacuo, yielding a beige solid. The compound was washed with cold hexane (−50 °C, 2 × 3 mL), affording complex **10** as an off-white solid. X-ray quality crystals were obtained by cooling a saturated hexane solution to −50 °C. Yield: 320 mg (86%). Anal. Calcd for $C_{30}H_{36}N_2NiO_3$ (MW 531.31): C, 67.82; H, 6.83; N, 5.27. Found: C, 67.55; H, 6.76; N, 5.09. ^{1}H NMR (C_6D_6, 400 MHz, δ): 7.02−7.16 (m, 6H, IPr−CH−Ar), 6.50 (s, 2H, NCH=CHN), 2.70 (septet, 4H, IPr−CH), 1.25 (d, 12H, IPr−CH3), 0.94 (d, 12H, IPr−CH3). ^{13}C NMR (C_6D_6, 100.6 MHz, δ): 198.21 (s, N−C−N), 197.64 (s, CO), 146.36 (s, IPr−C), 138.09 (s, IPr−C), 130.58 (s, IPr−C), 124.57 (s, IPr−C), 123.73 (s, NCH=CHN), 29.05 (s, IPr−CH), 25.79 (s, IPr−CH_3), 23.09 (s, IPr−CH_3), 17.93. IR ν_{CO} (hexane, cm^{-1}): 2055.1 (s), 1980.4 (vs), 1972.3 (vs). IR ν_{CO} (CH_2Cl_2, cm^{-1}): 2051.5 (s), 1970.0 (vs).

Synthesis of Ni(CO)$_3$SIPr (11). A THF solution (5 mL) of Ni(CO)$_4$ (143 mg, 0.84 mmol) was added to a stirred THF solution (5 mL) containing SIPr (272 mg, 0.70 mmol). The resulting pale yellow solution was left stirring at room temperature for 2 h, and then the volatiles were removed in vacuo, yielding a beige solid. The compound was washed with cold hexane (−45 °C, 2 × 3 mL), affording 312 mg (84% yield) of the desired complex. X-ray quality crystals were obtained by cooling a saturated hexane solution to −50 °C. Anal. Calcd for $C_{30}H_{38}N_2NiO_3$ (MW 533.33): C, 67.56; H, 7.18; N, 5.25. Found: C, 67.31; H, 7.20; N, 5.08. ^{1}H NMR (C_6D_6, 400 MHz, δ): 7.22−7.37 (m, overlapping with C_6D_6, 6H, SIPr−C**H**−Ar), 3.59 (s, 4H, NC**H**$_2$C**H**$_2$N), 3.32 (septet, 4H, SIPr−C**H**), 1.52 (d, 12H, J = 7.2 Hz, SIPr−C**H**$_3$), 1.25 (d, 12H, J = 6.8 Hz, SIPr−C**H**$_3$). ^{13}C NMR (C_6D_6, 100.6 MHz, δ): 223.16 (s, small, N−**C**−N), 198.16 (s, **C**O), 147.47 (s, SIPr−**C**), 138.65 (s, SIPr−**C**), 129.82 (s, SIPr−**C**), 125.09 (s, SIPr−**C**), 53.62 (s, N**C**H$_2$**C**H$_2$N), 29.09 (s, SIPr−**C**H), 26.25 (s, SIPr−**C**H$_3$), 24.10 (s, SIPr−**C**H$_3$). IR ν_{CO} (hexane, cm^{-1}): 2056.0 (s), 1982.6 (vs), 1973.7 (vs). IR ν_{CO} (CH_2Cl_2, cm^{-1}): 2052.2 (s), 1971.3 (vs).

Synthesis of Ni(CO)$_3$(ICy) (12). Addition of a hexane solution (5 mL) containing ICy (240 mg, 1.033 mmol) to a hexane solution (5 mL) of Ni(CO)$_4$ (229 mg, 1.343 mmol) under stirring led to the evolution of CO, and the resulting brownish solution was stirred at room temperature for 2 h. Slow evaporation of the solvent resulted in a color change to blue. The solid was washed with cold pentane (−50 °C, 2 × 3 mL), affording complex **12** as a blue powder. X-ray quality crystals were obtained by cooling a saturated pentane solution to −50 °C. Yield: 340 mg (88%). Anal. Calcd for $C_{18}H_{24}N_2NiO_3$ (MW 374.11): C, 57.64; H, 6.45; N, 7.47. Found: C, 57.86; H, 6.58; N, 7.43. ^{1}H NMR (C_6D_6, 400 MHz, δ): 6.53 (s, 2H, N**C**H=**C**HN), 4.68 (m, 2H, C**H**−Cy), 1.85 (d, 4H, J = 10.0 Hz, C**H**$_2$−Cy), 1.54 (d, 4H, J = 12.8 Hz, C**H**$_2$−Cy), 1.44 (d, 2H, J = 12.4 Hz, C**H**$_2$−Cy), 1.27 (m, 4H, C**H**$_2$−Cy), 1.12 (m, 4H, C**H**$_2$−Cy), 0.88 (m, 2H, C**H**$_2$−Cy). ^{13}C NMR (C_6D_6, 100.6 MHz, δ): 199.48 (s, N−**C**−N), 188.04 (s, **C**O), 117.39 (s, N**C**H=**C**HN), 60.10 (s, **C**H−Cy), 34.35 (s, **C**H$_2$−Cy), 26.08 (s, **C**H$_2$−Cy), 25.87 (s, **C**H$_2$−Cy). IR ν_{CO} (hexane, cm^{-1}): 2052.4 (s), 1973.4 (vs), 1968.0 (vs). IR ν_{CO} (CH_2Cl_2, cm^{-1}): 2049.6 (s), 1964.6 (vs).

Synthesis of Ni(CO)$_2$IAd (13). Slow addition of a hexane solution (15 mL) containing IAd (1768 mg, 5.253 mmol) to a hexane (15 mL) solution of Ni(CO)$_4$ (1166 mg, 6.829 mmol) under stirring led to evolution of CO and a color change to orange. The resulting solution was stirred at room temperature for 2 h during which time an orange precipitate formed. The solvent was evaporated, and the solid was washed with cold pentane (−50 °C, 2 × 7 mL), affording complex **13** as an orange powder. Yield: 2257 mg (95%). X-ray quality crystals were obtained by slow evaporation of a saturated diethyl ether solution containing **13**. Anal. Calcd for $C_{25}H_{32}N_2NiO_2$ (MW 451.23): C, 66.54; H, 7.15; N, 6.21. Found: C, 66.21; H, 7.48; N, 6.17. ^{1}H NMR (C_6D_6,

(26) Arduengo, A. J., III; Krafczyk, R.; Schmutzler, R.; Craig, H. A.; Goerlich, J. R.; Marshall, W. J.; Unverzagt, M. *Tetrahedron* **1999**, *55*, 14523−14534.

400 MHz, δ): 6.75 (s, 2H, NC**H**=C**H**N), 2.28 (s, 12H, IAd−C**H**$_2$), 1.93 (s, 6H, IAd−C**H**), 1.50 (m, 12H, IAd−C**H**$_2$). ^{13}C NMR(C_6D_6, 100.6 MHz, δ): 198.17 (s), 188.05 (s), 116.12 (s), 57.56 (s), 43.39 (s), 36.41 (s), 30.42 (s). IR ν_{CO} (hexane, cm^{-1}): 2007.2 (s), 1926.3 (vs).

Synthesis of Ni(CO)$_2$I^{t}Bu (14). Dropwise addition of a hexane solution (17 mL) containing I^{t}Bu (1000 mg, 5.54 mmol) to a hexane solution (3 mL) of Ni(CO)$_4$ (1230 mg, 7.20 mmol) under stirring led to the evolution of CO and a color change from colorless to orange. The solution was stirred at room temperature for 2 h, resulting in partial precipitation of a red solid. Subsequently, the volatiles were removed in vacuo, yielding a red solid, and the compound was washed with cold pentane (−50 °C, 2 × 10 mL), affording the desired complex **14** as a red solid. X-ray quality crystals were obtained by slow evaporation of a saturated pentane solution containing **14**. Yield: 1.57 g (96%). Anal. Calcd for $C_{13}H_{20}N_2NiO_2$ (MW 295.00): C, 52.93; H, 6.83; N, 9.50. Found: C, 52.08; H, 6.94; N, 9.38. ^{1}H NMR (C_6D_6, 400 MHz, δ): 6.60 (s, 2H, NC**H**=C**H**N), 1.40 (m, 18H, I^{t}Bu−C**H**$_3$). ^{13}C NMR (C_6D_6, 100.6 MHz, δ): 198.17 (s), 189.48 (s), 117.38 (s), 57.16 (s), 30.24 (s). IR ν_{CO} (hexane, cm^{-1}): 2009.7 (s), 1928.6 (vs).

Synthesis of Ni(CO)(C$_3$H$_3$F$_3$)(I^{t}Bu) (15). A pentane solution (12 mL) of Ni(CO)$_2$(I^{t}Bu) (**14**) (200 mg, 0.678 mmol) was treated with an excess of gaseous trifluoropropene. The solution turned yellow immediately with concomitant evolution of CO. The yellow solution was stirred for 30 min. The volatiles were evaporated in vacuo, yielding a yellow powder which was washed with small portions of cold pentane to give the desired complex **15** as a yellow solid. Yield: 214 mg (87%). Anal. Calcd for $C_{15}H_{23}N_2NiOF_3$ (MW 363.05): C, 49.63; H, 6.39; N, 7.72. Found: C, 49.69; H, 6.55; N, 7.44. ^{19}F NMR (C_6D_6, 376.3 MHz, δ): 40.55 (s). ^{1}H NMR (C_6D_6, 500 MHz, δ): 6.59 (s, 1H, NC**H**=C**H**N), 3.67 (dd, J = 12.0 and 8.7 Hz, 1H, CH$_2$=C**H**CF$_3$), 2.06 (d, J = 12.5 Hz, 1H, C**H**$_2$=CHCF$_3$), 1.71 (d, J = 9.0 Hz, 1H, C**H**$_2$=CHCF$_3$), 1.34 (s, 9H, I^{t}Bu−C**H**$_3$), 1.27 (s, 9H, I^{t}Bu−C**H**$_3$). ^{13}C NMR (C_6D_6, 125.6 MHz, δ): 196.13 (s), 190.18 (s), 118.29 (d, J = 10.8 Hz, N**C**H=CHN), 57.63 (d, J = 12.8 Hz), 49.93 (q, J = 34.5 Hz), 38.84 (d, J = 3.1 Hz), 31.28 (s, I^{t}Bu−**C**H$_3$), 31.14 (s, I^{t}Bu−**C**H$_3$). IR ν_{CO} (CH_2Cl_2, cm^{-1}): 1982.0 (vs).

Synthesis of NiCl(C$_3$H$_5$)(I^{t}Bu) (16). Addition of a pentane solution (4 mL) containing allyl chloride (154 mg, 2.034 mmol) to a pentane solution (12 mL) of Ni(CO)$_2$(I^{t}Bu) (**14**) (200 mg, 0.678 mmol) led to instant precipitation of a flaky, yellow solid. Leaving the flask under a stream of argon led to evolution of CO and to a heavy orange precipitate within 5 min. The suspension was stirred at room temperature for 2 h, decanted, and washed with pentane (2 × 3 mL). Subsequently, the volatiles were removed in vacuo, yielding the desired complex **16** as an orange solid. X-ray quality crystals were obtained by slow evaporation of an acetone solution. Yield: 207 mg (97%). Anal. Calcd for $C_{14}H_{25}ClN_2Ni$ (MW 330.54): C, 53.29; H, 7.99; N, 8.87. Found: C, 52.85; H, 8.15; N, 8.49. ^{1}H NMR (C_6D_6, 400 MHz, δ): 6.62 (s, 1H, NC**H**=CHN), 6.55 (s, 1H, NCH=C**H**N), 5.11 (m, 1H), 3.67 (d, J = 10.4 Hz, 1H), 2.98 (d, J = 18.8 Hz, 1H), 2.14 (d, J = 8.8 Hz, 1H), 1.94 (s, 9H, I^{t}Bu−C**H**$_3$), 1.66 (s, 9H, I^{t}Bu−C**H**$_3$), 1.22 (d, J = 16.8 Hz, 1H). ^{13}C NMR (C_6D_6, 100.6 MHz, δ): 179.93 (s, N−**C**−N), 119.32 (s, I^{t}Bu−N**C**H=CHN), 106.20 (s), 65.97 (s), 58.98 (s, I^{t}Bu−**C**), 58.55 (s, I^{t}Bu−**C**), 43.77 (s), 32.49 (s, I^{t}Bu−**C**H$_3$), 32.08 (s, I^{t}Bu−**C**H$_3$).

Synthesis of NiBr(C$_3$H$_5$)(I^{t}Bu) (17). Addition of a pentane solution (4 mL) containing allyl bromide (246 mg, 2.034 mmol) to a pentane solution (12 mL) of Ni(CO)$_2$(I^{t}Bu) (**14**) (200 mg, 0.678 mmol) led to instant precipitation of a flaky, yellow solid. After a few seconds, evolution of CO and precipitation of a yellow-orange solid were observed. The suspension was stirred at room temperature for 2 h, decanted, and washed with pentane (2 × 3 mL). Subsequently, the volatiles were removed in vacuo, yielding the desired complex **17** as an orange solid. X-ray quality crystals were obtained by slow evaporation of an acetone solution. Yield: 114 mg (93%). ^{1}H NMR (C_6D_6, 500 MHz, δ): 6.60 (s, 1H, NC**H**=CHN), 6.53 (s, 1H, NCH=C**H**N), 5.02 (sept, J = 6.5 Hz, 1H), 3.74 (d, J = 7.0 Hz, 1H), 2.87 (d, J = 14.0 Hz, 1H), 2.32 (d, J = 6.5 Hz, 1H), 1.90 (s, 9H, I^{t}Bu−C**H**$_3$), 1.63 (s, 9H, I^{t}Bu−C**H**$_3$), 1.29 (d, J = 12.0 Hz, 1H). ^{13}C NMR (C_6D_6, 100.6 MHz, δ): 179.36 (s, N−**C**−N), 119.65 (s, N**C**H=CHN), 119.59 (s, NCH=**C**HN), 105.61(s), 64.88 (s), 58.91 (s, I^{t}Bu−**C**), 58.51 (s, I^t-Bu−**C**), 46.50 (s), 32.36 (s, I^{t}Bu−**C**H$_3$), 31.97 (s, I^{t}Bu−**C**H$_3$).

Synthesis of NiCl(C$_3$H$_5$)(IAd) (18). A pentane solution (10 mL) of Ni(CO)$_2$(IAd) (**13**) (60 mg, 0.133 mmol) was added to allyl chloride (31 mg, 0.399 mmol) leading to slow formation of a flaky, yellowish precipitate. The suspension was stirred under argon at room temperature for 6 h, during which time a pale precipitate formed. The pentane solution was decanted, the solid washed with additional pentane (3 × 5 mL), and dried in vacuo, yielding the desired complex **18** as a pale orange solid. Yield: 61 mg (98%). ^{1}H NMR (C_6D_6, 400 MHz, δ): 6.82 (s, 1H, NC**H**=CHN), 6.74 (s, 1H, NCH=C**H**N), 5.29 (m, 1H), 3.70 (d, J = 7.6 Hz, 1H), 3.07−1.50 (different d and m, 32H), 1.37 (d, J = 12.0 Hz, 1H). ^{13}C NMR (C_6D_6, 100.6 MHz, δ): 179.01 (s, N−**C**−N), 118.03 (d, J = 4.8 Hz, N**C**H=CHN), 105.68 (s), 65.52 (s), 59.78 (s, IAd−**C**), 59.30 (s, IAd−**C**), 44.93 (s, IAd−**C**H), 44.56 (s, IAd−**C**H), 44.47 (s), 36.60 (s, IAd−**C**H$_2$), 36.53 (s, IAd−**C**H$_2$), 30.77 (s, IAd−**C**H$_2$), 30.66 (s, IAd−**C**H$_2$).

Synthesis of NiBr(C$_3$H$_5$)(IAd) (19). Addition of a pentane solution (5 mL) containing allyl bromide (48 mg, 0.399 mmol) to a pentane solution (5 mL) of Ni(CO)$_2$(IAd) (**13**) (60 mg, 0.133 mmol) led to the precipitation of a flaky, yellow solid within 20 min. The suspension was stirred at room temperature for 5 h, decanted, and washed with pentane (3 × 5 mL). Subsequently, the volatiles were removed in vacuo, yielding the desired complex **19** as a pale orange solid. Yield: 64 mg (93%). ^{1}H NMR (C_6D_6, 400 MHz, δ): 6.83 (s, 1H, NC**H**=CHN), 6.75 (s, 1H, NCH=C**H**N), 5.20 (septet, J = 6.4 Hz, 1H), 3.76 (d, J = 6.4 Hz, 1H), 2.94 (d, J = 14.0 Hz, 1H), 3.07−1.50 (different d and m, 31H), 1.44 (d, J = 12.4 Hz, 1H). ^{13}C NMR (C_6D_6, 100.6 MHz, δ): 178.59 (s, N−**C**−N), 118.32 (s, N**C**H=CHN), 105.11 (s), 64.49 (s), 59.78 (s, IAd−**C**), 59.34 (s, IAd−**C**), 47.23 (s), 44.82 (s, IAd−**C**H), 44.51 (s, IAd−**C**H), 36.56 (s, IAd−**C**H$_2$), 36.50 (s, IAd−**C**H$_2$), 30.73 (s, IAd−**C**H$_2$), 30.64 (s, IAd−**C**H$_2$).

Computational Details. The Amsterdam Density Functional (ADF) program was used to obtain all of the results discussed herein.[27,28] The electronic configuration of the molecular systems was described by a triple-ζ STO basis set on nickel for 3s, 3p, 3d, 4s, and 4p (ADF basis set IV).[25] Double-ζ STO basis sets were used for phosphorus (3s, 3p), oxygen, nitrogen, and carbon (2s,2p) and hydrogen (1s) augmented with single 4d, 3d, 3d, 3d, and 2p functions, respectively (ADF basis set III).[25] The inner shells on nickel and phosphorus (including 2s, 2p), oxygen, nitrogen, and carbon (1s), were treated within the frozen core approximation. Energies and geometries were evaluated using the local exchange−correlation potential by Vosko et al.,[29] augmented in a self-consistent manner with Becke's[30] exchange gradient correction and Perdew's[31,32] correlation gradient correction.

The ADF program was modified by one of us[33,34] to include standard molecular mechanics force fields in such a way that the QM and MM parts are coupled self-consistently.[32,35] The simple model QM systems and the full QM/MM and QM systems are displayed in Figure 14. The partitioning of the systems into QM and MM parts only involves the NHC ligand. Specifically, the N-bonded R groups are treated as MM atoms.

(27) *ADF 2003*, User's Manual; Vrije Universiteit Amsterdam: Amsterdam, The Netherlands, 2003.
(28) te Velde, G.; Bickelhaupt, F. M.; Baerends, E. J.; Fonseca Guerra, C.; Van Gisbergen, S. J. A.; Snijders, J. G.; Ziegler, T. *J. Comput. Chem.* **2001**, *22*, 931−967.
(29) Vosko, S. H.; Wilk, L.; Nusair, M. *Can. J. Phys.* **1980**, *58*, 1200−1211.
(30) Becke, A. D. *Phys. Rev. A* **1988**, *38*, 3098−3100.
(31) Perdew, J. P. *Phys. Rev. B* **1986**, *33*, 8822−8824.
(32) Perdew, J. P. *Phys. Rev. B* **1986**, *34*, 7406−7408.
(33) Cavallo, L.; Woo, T. K.; Ziegler, T. *Can. J. Chem.* **1998**, *76*, 1457−1466.
(34) Woo, T. K.; Cavallo, L.; Ziegler, T. *Theor. Chim. Acta* **1998**, *100*, 307−313.
(35) Maseras, F.; Morokuma, K. *J. Comput. Chem.* **1995**, *16*, 1170−1179.

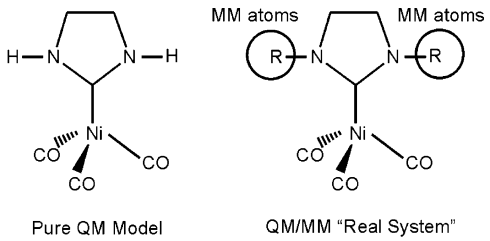

Figure 14. Representation of the partitioning of the systems into QM and MM regions.

As for the connection between the QM and MM parts, this occurs by means of the so-called "capping" dummy atoms, which are replaced in the real system by the corresponding "linking" atom.[32,33] H atoms were used as capping atoms for all of the N−C linking bonds. In the QM/MM optimizations, the ratio between the N−C bonds crossing the QM/MM border and the corresponding optimized N−H distance was fixed to 1.36. The AMBER95 force field[36] was used for the MM potentials, except for Ni, which was treated with the UFF force field.[37] To eliminate spurious stabilizations from the long-range attractive part of the Lennard-Jones potential,[38,39] we used an exponential expression fitted to the repulsive part of the Lennard-Jones potential.[40,41]

The minima were localized by full optimization of the starting structures. Convergence criterion in the geometry optimizations was set to 2×10^{-3} a.u. on the maximum Cartesian gradient.

Acknowledgment. The National Science Foundation is gratefully acknowledged for financial support of this work. Dr. Kenneth Moloy and DuPont CR&D are especially thanked for the gift of $Ni(CO)_4$. We thank Eli Lilly and Co. and the Lonza Group for generous donation of amines. L.C. thanks the University of Salerno for financial support (Grant Piccole di Ateneo 2002).

Supporting Information Available: Crystallographic information files (CIF) of complexes **8**−**11**, **16**, and **17**. Crystallographic data have been deposited at the CCDC, 12 Union Road, Cambridge CB2 1EZ, U.K., and can be obtained on request, free of charge, by quoting the publication citation and the deposition number 252129 (**8**), 252130 (**9**), 252131(**10**), 252132(**11**), 252133(**16**), 252134(**17**). This material is available free of charge via the Internet at http://pubs.acs.org.

JA0438821

(36) Cornell, W. D.; Cieplak, P.; Bayly, C. I.; Gould, I. R.; Merz, K. M. J.; Ferguson, D. M.; Spellmeyer, D. C.; Fox, T.; Caldwell, J. W.; Kolmann, P. A. *J. Am. Chem. Soc.* **1995**, *117*, 5179−5197.
(37) Rappé, A. K.; Casewit, C. J.; Colwell, K. S.; Goddard, W. A., III; Shiff, W. M. *J. Am. Chem. Soc.* **1992**, *114*, 10024−10035.
(38) Sauers, R. R. *J. Chem. Educ.* **1996**, *73*, 114−116.
(39) Lee, K. J.; Brown, T. L. *Inorg. Chem.* **1992**, *31*, 289−294.
(40) Woo, T. K.; Ziegler, T. *Inorg. Chem.* **1994**, *33*, 1857−1863.
(41) Guerra, G.; Cavallo, L.; Corradini, P.; Longo, P.; Resconi, L. *J. Am. Chem. Soc.* **1997**, *119*, 4394−4403.